2011 International Conference on Computer Science and Information Technology (ICCSIT 2011)
IPCSIT vol. 51 (2012) © (2012) IACSIT Press, Singapore
DOI: 10.7763/IPCSIT.2012.V51.71

The Split-Bregman-Projection Algorithm of a Variational Model for Multiphase Image Segmentation

Cunliang Liu[a,b,+], Yongguo Zheng[a], Zhenkuan Pan[b], Guodong Wang[b]

[a]College of Information Science & Engineering Shandong University of Science & Technology, Qingdao 266510, China

[b]College of Information Engineering, Qingdao University, Qingdao 266071, China

Abstract. In this paper, we propose a variational model for multiphase image segmentation by using n binary label functions to partition n regions. Our proposed model is subjected to n constraints due to the definition of binary functions and a constraint for avoidance of vacuum and overlapping. We use the convex relaxation approach to solve binary constraints of label functions. In order to satisfy the constraint of the second class, we develop the projection algorithm based on Lagrange multiplier method. To improve its computation efficiency, we design the Split Bregman algorithm for solution of every label function after convexification of it during alternating minimization. 2D and 3D multiphase image segmentation experiments are given to validate our model and the Split-Bregman-Projection algorithm.

Keywords: active contour model, multiphase segmentation, Split Bregman, Lagrangian multiplier

1. Introduction

Segmentation is an important problem in image processing and computer vision. Its aim is to partition an image into a finite number of semantically important regions. Many of the most general segmentation methods can be written as variational based models such as the well-known active contour model, initially proposed by Kass et al. [1]. Edge-based segmentation models and region-based ones are both effective active contour models. Our proposed algorithm takes a region-based active contour method. One of the early efforts towards region-based models was made by the Mumford and Shah model [4]. However, the energy minimization problem in [4] is difficult to solve. Chan and Vese [5] proposed a two-phase piecewise constant segmentation model, which was called the "active contours without edges" (ACWE) model. The ACWE model is a simplified version of the Mumford and Shah model. Chan and Vese chose the level set method [3] to represent the evolving curve.

Multiphase segmentation models are considered the extension from two-phase segmentation models, and several attempts have been made towards this extension. Samson et al.'s [6] model represented n regions by n level set functions. Vese and Chan [7] used n level set functions to represent 2n regions. Pan et al. [8] used n-1 level set functions to represent n phases. One level set formulation can also represent n regions [9]-[10].

Despite many good numerical results obtained with the level set evolution methods, region-based models to segmentation suffer from two major difficulties. The first is that neither model is globally convex. The second is that these traditional contour evolution schemes based on the PDE approach require the users to re-initialize the level set function, which is time consuming.

+ Corresponding author.
E-mail address: clliuqdu@gmail.com.

To resolve the two problems, several new models have been proposed. Chan et al. [11] proposed a convexification of the ACWE model. Build on [11], Bresson et al. [12] proposed a fast global minimization based on a dual formulation. Goldstein et al. [13] proposed a fast globally convex segmentation on the basis of the Split Bregman algorithm [14]. These convex models introduced above are designed for the two-phase segmentation. Furthermore, the authors [15]-[17] also attempted to propose the global minimization methods for multiphase image segmentation.

In this paper, we propose the Split-Bregman-Projection algorithm for multiphase image segmentation. The outline of the paper is as follows. In Section II, we review some related works. Our proposed segmentation method is introduced in Section III. The implementation and experimental results are shown in Section IV. This paper is summarized in Section V.

2. Fast global minimization of two-phase piecewise constant segmentation model

2.1. Globally convex segmentation models

Let $\Omega \subset \Re^N$ be the image domain, $u_0 : \Omega \to \Re$ be a given image. The variable X in $u_0(X)$ is a point in Ω. Using the Heaviside function H, the ACWE model can be represented in the following level set formulation

$$\min_{\Phi, c_1, c_2} \left\{ E_{ACWE} = \gamma \int_\Omega |\nabla H(\Phi)| dX + \int_\Omega \alpha_1 (c_1 - u_0)^2 H(\Phi) dX + \int_\Omega \alpha_2 (c_2 - u_0)^2 (1 - H(\Phi)) dX \right\} \tag{1}$$

The minimization of (1) can be solved by the standard PDE method. The flow of E_{ACWE} is

$$\frac{\partial \Phi}{\partial t} = \delta(\Phi) \left(\gamma \nabla \cdot \left(\frac{\nabla \Phi}{|\nabla \Phi|} \right) - \left(\alpha_1 (c_1 - u_0)^2 - \alpha_2 (c_2 - u_0)^2 \right) \right) \tag{2}$$

where δ is the Delta function with $H' = \delta$.

As we previously said, the level set minimization problem is a non-convex energy minimization problem. Chan et al. [11] proposed a convex method of the ACWE model, which we call the globally convex segmentation (GCS) model. We remind the general ideas.

Since $\delta(\Phi) \geq 0$, we remove the Dirac function of (2) without changing the optimality condition. This simplified flow is as follows

$$\frac{\partial \Phi}{\partial t} = \gamma \nabla \cdot \left(\frac{\nabla \Phi}{|\nabla \Phi|} \right) - \left(\alpha_1 (c_1 - u_0)^2 - \alpha_2 (c_2 - u_0)^2 \right) \tag{3}$$

The flow (3) represents the gradient descent for minimizing the energy

$$\min_{c_1, c_2, \phi \in \{0,1\}} \left\{ E^1_{GCS} = \gamma \int_\Omega |\nabla \phi| dX + \int_\Omega \alpha_1 (c_1 - u_0)^2 \phi dX + \int_\Omega \alpha_2 (c_2 - u_0)^2 (1 - \phi) dX \right\} \tag{4}$$

where function ϕ is a binary label function [11] $(i.e. \phi \in \{0,1\})$. We change the notation Φ into ϕ to avoid any confusion with the level set function here. By relaxing the binary constraint of the label function ϕ over the interval [0, 1], we get the convex minimization problem

$$\min_{c_1, c_2, \phi \in [0,1]} \left\{ E^2_{GCS} = \gamma \int_\Omega |\nabla \phi| dX + \int_\Omega \alpha_1 (c_1 - u_0)^2 \phi dX + \int_\Omega \alpha_2 (c_2 - u_0)^2 (1 - \phi) dX \right\} \tag{5}$$

Based on the approach of Chan et al. [11], Bresson et al. [12] proposed the enhanced convex energy

$$\min_{c_1, c_2, \phi \in [0,1]} \left\{ E^g_{GCS} = \gamma \int_\Omega g(u_0) |\nabla \phi| dX + \int_\Omega \alpha_1 (c_1 - u_0)^2 \phi dX + \int_\Omega \alpha_2 (c_2 - u_0)^2 (1 - \phi) dX \right\} \tag{6}$$

The difference between energy (6) and energy (5) is the introduction of an edge detector function g(u0) [2]. One common choice for the edge detector is

$$g(u_0) = \frac{1}{1 + |\nabla G_\sigma * u_0|^2} \tag{7}$$

where G_σ is a Gaussian kernel and $G_\sigma * u_0$ is a smoother alternative to u0. Besides improving the regularization process of the ACWE model, Energy (6) provides a GCS model.

2.2. The Split Bregman algorithm

The Split Bregman algorithm was initially introduced for solving general L1-norm problems [14]. In [13], this method was applied to the GCS problem. We give a brief overview of this technique here.

We first introduce the auxiliary variable $\vec{d} \leftarrow \nabla\phi$, the energy (6) becomes

$$\min_{\vec{d},c_1,c_2,\phi\in[0,1]} \left\{ E^g_{GCS} = \gamma \int_\Omega g(u_0)\left|\vec{d}\right| dX + \int_\Omega \alpha_1 (c_1 - u_0)^2 \phi dX + \int_\Omega \alpha_2 (c_2 - u_0)^2 (1-\phi) dX \right\} \tag{8}$$

To approximately enforce these equality constraints, we then add quadratic penalty functions and get the following unconstrained problem

$$\min_{\vec{d},c_1,c_2,\phi\in[0,1]} \left\{ \begin{array}{l} E^g_{GCS} = \gamma \int_\Omega g(u_0)\left|\vec{d}\right| dX + \frac{\theta}{2}\left(\vec{d} - \nabla\phi\right)^2 \\ \qquad + \int_\Omega \alpha_1 (c_1 - u_0)^2 \phi dX + \int_\Omega \alpha_2 (c_2 - u_0)^2 (1-\phi) dX \end{array} \right\} \tag{9}$$

In order to exactly enforce the constraint $\vec{d} = \nabla\phi$, we finally apply Bregman iteration to the unconstrained problem (9) by adding a vector, b, inside of the quadratic penalty function. The resulting sequence of optimization problems is

$$\left(\phi^{k+1}, \vec{d}^{\,k+1}\right) = \arg\min_{\phi,\vec{d},\phi\in[0,1]} \left\{ \begin{array}{l} \gamma \int_\Omega g(X)\left|\vec{d}\right| dX + \frac{\theta}{2}\left(\vec{d} - \nabla\phi - \vec{b}^{\,k+1}\right)^2 \\ + \int_\Omega \alpha_1 (c_1 - u_0)^2 \phi dX + \int_\Omega \alpha_2 (c_2 - u_0)^2 (1-\phi) dX \end{array} \right\} \tag{10}$$

where $\vec{b}^{k+1} = \vec{b}^{k} + \nabla\phi^k - \vec{d}^{k}$. See [13] for more details.

3. The Split-Bregman-Projection method

3.1. The proposed energy

Samson et al. proposed the following level set energy minimization problem

$$\min_{c,\Phi} \left\{ E_{n2n} = \sum_{i=1}^{n} \gamma_i \int_\Omega g(u_0)\delta(\Phi_i)|\nabla\Phi_i| dX + \sum_{i=1}^{n} \alpha_i \int_\Omega (c_i - u_0)^2 H(\Phi_i) dX + \frac{\lambda}{2}\int_\Omega \left(\sum_{i=1}^{n} H(\Phi_i) - 1\right)^2 dX \right\} \tag{11}$$

where the first term of the right-hand side of (11) is used to enforce the regularity of the interface. The second term is a data fidelity term, and the third one is the constraints on no vacuum and overlapping of regions. For a more precise statement of this model, we refer the reader to [6].

Based on [11]-[13], we replace the level set functions $\Phi_i, i = 1...n,$ by the label functions $\phi_i, i = 1,...,n.$ Hence our new model is to minimize the following energy

$$\min_{c,\phi} \left\{ E^c_{n2n} = \sum_{i=1}^{n} \gamma_i \int_\Omega g(u_0)|\nabla\phi_i| dX + \sum_{i=1}^{n} \alpha_i \int_\Omega (c_i - u_0)^2 \phi_i dX \right\} \tag{12}$$

where the label function ϕ_i satisfies two constraints

$$K(\phi_i) = \phi_i(\phi_i - 1) = 0 \quad (\text{i.e., } \phi_i \in \{0,1\}) \tag{13}$$

and

$$L(\phi) = \sum_{i=1}^{n} \phi_i - 1 = 0 \tag{14}$$

Let us rewrite the problem (12) as

$$\min_{c,\phi,K(\phi_i)=0,L(\phi)=0} \left\{ E^c_{n2n} = \sum_{i=1}^{n} \gamma_i \int_\Omega g(u_0)|\nabla\phi_i| dX + \sum_{i=1}^{n} \alpha_i \int_\Omega (c_i - u_0)^2 \phi_i dX \right\} \tag{15}$$

3.2. Energy minimization

We now turn to an alternative way of carrying out the constrained minimization problem (15). First we consider the unconstrained problem

$$\min_{c,\tilde{\phi},K(\phi_i)=0} \left\{ E^{c1}_{n2n} = \sum_{i=1}^{n} \gamma_i \int_\Omega g(u_0)\left|\nabla\tilde{\phi}_i\right| dX + \sum_{i=1}^{n} \alpha_i \int_\Omega (c_i - u_0)^2 \tilde{\phi}_i dX \right\} \tag{16}$$

where $\tilde{\phi}$ are obtained without the constraint (14).

Then we use the Lagrangian multiplier method to project $\tilde{\phi}$ on ϕ_i. The functional is defined as

$$\min_{\lambda,\phi} \left\{ E^{c2}_{n2n} = \sum_{i=1}^{n} \int_\Omega \left(\phi_i - \tilde{\phi}_i^{\,k+1}\right)^2 dX + \lambda \int_\Omega L(\phi_i) dX \right\} \tag{17}$$

where λ is the multiplier.

3.3. Solving $\tilde{\phi}$

We relax constraint (13) by letting $\tilde{\phi}_i \in [0,1]$ and apply the Split Bregman method to E_{n2n}^{c1}

$$\left(\tilde{\phi}_i^{k+1}, \vec{d}_i^{k+1}\right) = \arg \min_{\tilde{\phi}, \vec{d}, \tilde{\phi}_i \in [0,1]} \left\{ \begin{array}{l} \sum_{i=1}^{n} \gamma_i \int_\Omega g(u_0) \left|\vec{d}_i\right| dX + \frac{\theta}{2} \sum_{i=1}^{n} \int_\Omega (\vec{d}_i - \nabla \tilde{\phi}_i - \vec{b}_i^{k+1})^2 dX \\ + \sum_{i=1}^{n} \alpha_i \int_\Omega (c_i - u_0)^2 \tilde{\phi}_i dX \end{array} \right\} \tag{18}$$

where $\vec{b}_i^{k+1} = \vec{b}_i^{k} + \nabla \tilde{\phi}_i^{k} - \vec{d}_i^{k}$. We use the alternative minimization method to find the numerical solution.

Firstly, we fix $\vec{d}_i^{k}$ to solve $\tilde{\phi}_i^{k+1}$:

$$\min_{\tilde{\phi}} \left\{ \frac{\theta}{2} \sum_{i=1}^{n} \int_\Omega (\vec{d}_i^{k} - \nabla \tilde{\phi}_i - \vec{b}_i^{k+1})^2 dX + \sum_{i=1}^{n} \alpha_i \int_\Omega \left(c_i^{k} - u_0\right)^2 \tilde{\phi}_i dX \right\} \tag{19}$$

The solution of (19) is given by the following PDE's

$$\left\{ \begin{array}{ll} \theta \nabla \cdot \left(\nabla \tilde{\phi}_i + \vec{b}_i^{k+1} - \vec{d}_i^{k} \right) - \alpha_i \left(c_i^{k} - u_0\right)^2 = 0 & in\ \Omega \\ \left(\nabla \tilde{\phi}_i + \vec{b}_i^{k+1} - \vec{d}_i^{k} \right) \cdot \vec{n} = 0 & on\ \partial\Omega \end{array} \right. \tag{20}$$

We obtain $\tilde{\phi}_i^{k+1}$ using a Gauss-Seidel method [13]. To ensure $\tilde{\phi}_i^{k+1} \in [0,1]$, we can use the following formula

$$\tilde{\phi}_i^{k+1} = \max\left(\min\left(\tilde{\phi}_i^{k+1}, 1\right), 0\right) \tag{21}$$

Secondly, we fix $\tilde{\phi}_i^{k+1}$ to solve $\vec{d}_i^{k+1}$:

$$\min_{\vec{d}} \left\{ \sum_{i=1}^{n} \gamma_i \int_\Omega g(u_0) \left|\vec{d}_i\right| dX + \frac{\theta}{2} \sum_{i=1}^{n} \int_\Omega (\vec{d}_i - \nabla \tilde{\phi}_i - \vec{b}_i^{k+1})^2 dX \right\} \tag{22}$$

Minimization with respect to $\vec{d}_i^{k+1}$ can be performed explicitly using the vector-valued shrinkage operator[18]

$$\vec{d}_i^{k+1} = \max\left\{ \left| \nabla \tilde{\phi}_i^{k+1} + \vec{b}_i^{k+1} \right| - \frac{\gamma_i}{\theta}, 0 \right\} \frac{\nabla \tilde{\phi}_i^{k+1} + \vec{b}_i^{k+1}}{\left| \nabla \tilde{\phi}_i^{k+1} + \vec{b}_i^{k+1} \right|} \tag{23}$$

3.4. Solving ϕ

The Euler-Lagrange equation of the energy functional (17) is as follows

$$\phi_i - \tilde{\phi}_i^{k+1} + \lambda = 0 \tag{24}$$

From (14) and (24), we get

$$\phi_i^{k+1} = \tilde{\phi}_i^{k+1} - \frac{\sum_{j=1}^{n} \tilde{\phi}_i^{k+1} - 1}{n} \tag{25}$$

The final segmented regions are found by thresholding the function ϕ_i to get

$$\left\{ X \in \Omega \mid \phi_i(X) > \mu \right\} \tag{26}$$

where $\mu \in (0,1)$.

4. Experimental results

We test our algorithm on synthetic and natural images which appear in the recent image segmentation literatures. The experiments are performed under Windows XP and MATLAB v7.0 with Intel Core 2 Duo CPU at 2.53 GHz and 2 GB of RAM. All the presented results are zoomed in.

Our first test demonstrates the advantages of our algorithm compared with the Samson et al.'s traditional algorithm. From Fig. 1 and Fig. 2, we show that our model improves the accuracy of segmentation. Besides, we find that the Split Bregman algorithm make the convergence faster than the traditional algorithm from table 1.

In Fig. 3, we test our method with four-phase image segmentation. The image in Fig. 3(a) is available to the public at http://www.bic.mni.mcgill.ca/brainweb/. There are four classes that should be identified: cerebrospinal fluid (CSF), gray matter (GM), white matter (WM) and the background. But we do not depict

the background phase here. Compared with the exact results in Fig. 3(f), (g) and (h), our results are satisfactory.

As a final test we consider the 3D data problem. The data presented on Fig. 4 are provided by The National Library of Medicine's Visible Human Project. We select 105 2D images as the original input data for the 3D segmentation and reconstruction. The size of each image is 150*128. There are three phases that should be identified: mandible, teeth and the background. Also, we do not depict the background phase here. As can be seen, our model is easy to extend to three-dimensional problems, and the results seem as good as for two-dimensional problems.

5. Conclusions

We have presented a variational model based on the labeling functions for multiphase segmentation. Also, we proposed an efficient and fast numerical scheme to minimize the variational segmentation model. For some applications, particularly when the data must be processed in "real time", the most important consideration when choosing a segmentation method is speed. Our proposed model, based on the Split-Bregman-Projection algorithm, is easy to implement and allow us to avoid the usual drawback in the level set approach to ensure a correct computation. The energy function for our approach is locally convex, which means that proper initial guesses are needed. Future works will find the good initial contours and investigate the extension of this global minimization approach to our model.

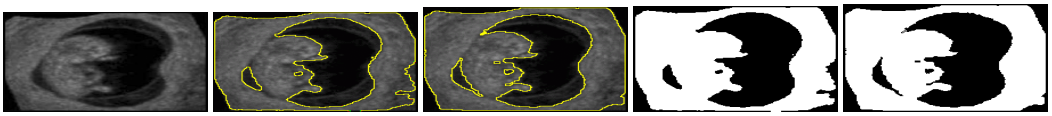

Fig. 1. Two-phase image segmentation; (a) ultrasound image with Rayleigh distribution; (b) the segmentation by the method in [6] ($\gamma_i = 90$, $\alpha_i = 0.015$, $\lambda = 200$); (c) the segmentation by our proposed method ($\gamma_i = 1500$, $\alpha_i = 0.2$, $\theta = 300$); (d) the level set function $H(\Phi_1)$ by the method in [6]; (e) the labeling function ϕ_1 by our proposed method; Image size is 180*170

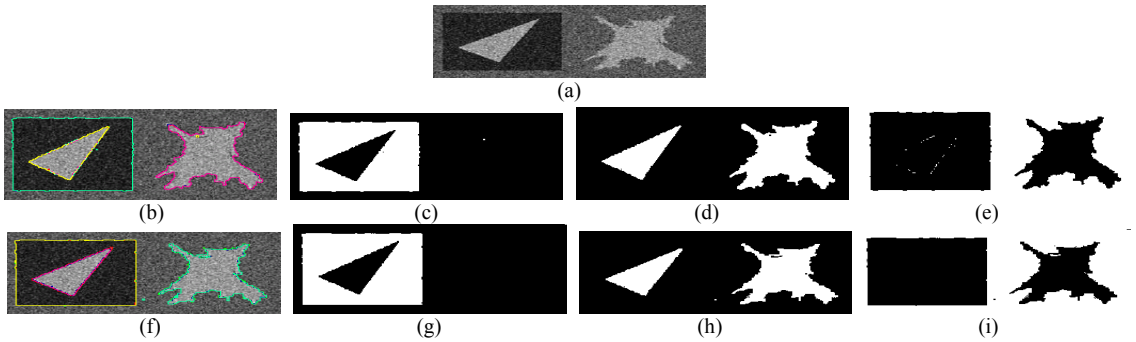

Fig. 2: Three-phase image segmentation; (a) synthetic image with Gaussian distribution; (b) the segmentation by the method in [6] ($\gamma_i = 90$, $\alpha_i = 0.015$, $\lambda = 300$); (f) the segmentation by our proposed method ($\gamma_i = 355$, $\alpha_i = 0.2$, $\theta = 400$); (c), (d) and (e) the three phases by the method in [6]; (g), (h) and (i) the classification results by our proposed method; Image size is 256*128

Tab.1： Iterations and computing time using different methods

Solving methods	Number of iterations		Time of iterations	
	Fig. 1	Fig. 2	Fig. 1	Fig. 2
The method [6]	380	680	13.315s	38.257s
Our method	5	15	0.197s	0.783s

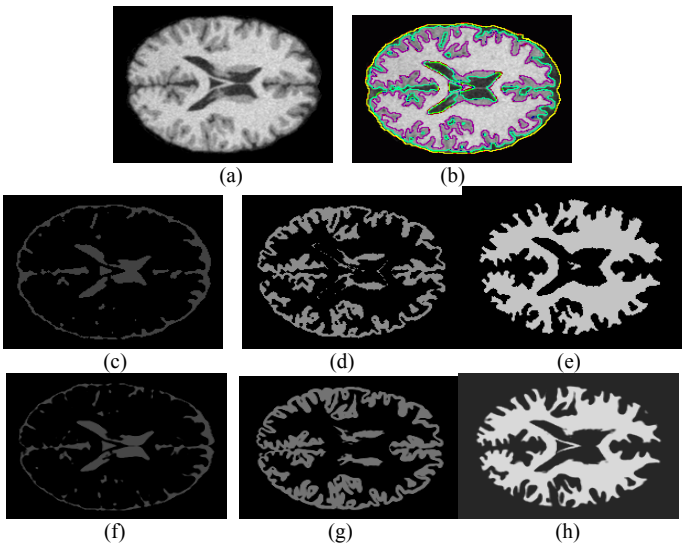

Fig. 3： Four-phase segmentation; (a) a brain MR image with noise 7% and RF-plus 20%; (b) the classification results by our proposed method ($\gamma_i = 0.01$, $\alpha_i = 0.1$, $\theta = 1500$, number of iterations = 10, total time of iterations = 0.688 seconds); (c), (d) and (e) three different tissues by our proposed method; (f), (g) and (h) the exact phases; Image size is 200*160

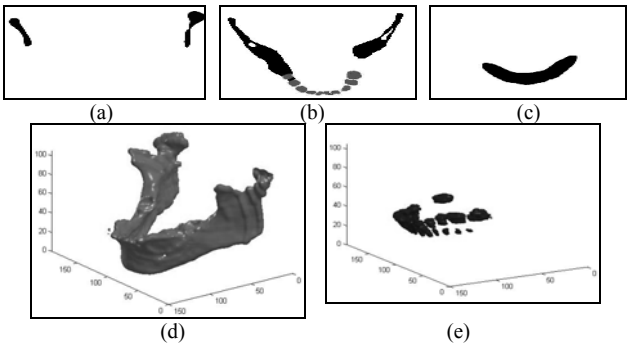

Fig. 4： 3D segmentation and reconstruction of mandible and teeth; (a)-(c) the 25th, 60th and 95th image; (d)-(e) the results of 3D segmentation and reconstruction by our method ($\gamma_i = 0.01$, $\alpha_i = 0.1$, $\theta = 1000$, iterations = 10, time = 57.359 seconds)

6. Acknowledgements

This work was supported in part by the National Natural Science Foundation of China (61170106) and in part by Natural Science Foundation of Shandong Province (ZR2010FQ030).

7. References

[1] Kass M, Witkin A, Terzopoulos D. Snakes: active contour models. *International Journal of Computer Vision* 1987; 1:321–331.

[2] Caselles V, Kimmel R, Sapiro G. Geodesic active contours. *International Journal of Computer Vision* 1997; 22:61–79.

[3] Osher S, Sethian J A. Fronts propagating with curvature-dependent speed: algorithms based on Hamilton–Jacobi formulation. *Journal of Computational Physics* 1988; 79:12–49.

[4] Mumford D, Shah J. Optimal Approximations of piecewise smooth functions and associated variational problems. *Communications on Pure and Applied Mathematics* 1989; 42:577–685.

[5] Chan T F, Vese L A. Active contours without edges. *IEEE Transactions on Image Processing* 2001; 10:266–277.

[6] Samson C, Blanc-Feraud L, Aubert G. A level set model for image classification. *International Journal of Computer Vision* 2000; 40:187-197.

[7] Vese L A, Chan T F. A multiphase level set framework for image segmentation using the Mumford and Shah model. *International Journal of Computer Vision* 2002; 50:271-293.

[8] Pan Z-K, Li H, Wei W-B, et al. A variational level set method of multiphase segmentation for 3D images. *Chinese Journal of Computers* 2009; 32:2464-2474.

[9] Chung G, Vese L A. Energy minimization based segmentation and denoising using a multilayer level set approach. *EMMCVPR05* 2005; 439-455.

[10] Lie J, Lysaker M, Tai X-C. A variant of the level set method and applications to image segmentation. *Mathematics of Computation* 2006; 75:1155–1174.

[11] Chan T F, Esedoglu S, Nikolova M. Algorithms for finding global minimizers of image segmentation and denoising Models. *SIAM Journal on Applied Mathematics* 2006; 66:1932-1648.

[12] Bresson X, Esedoglu S, Vandergheynst P, et al. Fast global minimization of the active contour/snake model. *Journal of Mathematical Imaging and Vision* 2007; 28:151–167.

[13] Goldstein T, Bresson X, Osher S. Geometric applications of the Split Bregman method: segmentation and surface reconstruction. *Journal of Scientific Computing* 2010; 45:272-293.

[14] Goldstein T, Osher S. The Split Bregman method for L1 regularized problems. *SIAM Journal on Imaging Sciences* 2008; 2:323-343.

[15] Ethan S B, Chan T F, Bresson X. A convex approach for multi-phase piecewise constant Mumford-Shah image segmentation. *UCLA CAM Report 09-66* 2009.

[16] Bae E, Yuan J, Tai X-C. Global minimization for continuous multiphase partitioning problems using a dual approach. *International Journal of Computer Vision* 2011; 92:112-129.

[17] Ethan S B, Chan T F, Bresson X. A convex relaxation method for a class of vector-valued minimization problems with applications to Mumford-Shah segmentation. *UCLA CAM Report 10-43*; 2010.

[18] Wang Y-L, Yin W-T, Zhang Y. A fast algorithm for image deblurring with total variation regularization. *CAAM Technical Reports 07-10* 2007.